Parkinson-related LRRK2 mutation R1441C/G/H impairs PKA phosphorylation of LRRK2 and disrupts its interaction with 14-3-3

Kathrin Muda[a], Daniela Bertinetti[a], Frank Gesellchen[b], Jennifer Sarah Hermann[a], Felix von Zweydorf[c], Arie Geerlof[d], Anette Jacob[e], Marius Ueffing[c,f], Christian Johannes Gloeckner[c,f,1], and Friedrich W. Herberg[a,1,2]

[a]Department of Biochemistry, University of Kassel, 34132 Kassel, Germany; [b]Division of Biomedical Engineering, School of Engineering, University of Glasgow, Glasgow G12 8LT, United Kingdom; [c]Medical Proteome Center, Institute for Ophthalmic Research, Eberhard Karls University Tübingen, 72074 Tübingen, Germany; [d]Institute of Structural Biology, Protein Expression and Purification Facility, Helmholtz Zentrum München, 85764 Neuherberg, Germany; [e]Functional Genome Analysis, Deutsches Krebsforschungszentrum, 69120 Heidelberg, Germany; and [f]Research Unit Protein Science, Helmholtz Zentrum München, 85764 Neuherberg, Germany

Edited* by Susan S. Taylor, University of California, San Diego, La Jolla, CA, and approved November 19, 2013 (received for review July 7, 2013)

Leucine-rich repeat kinase 2 (LRRK2) is a multidomain protein implicated in Parkinson disease (PD); however, the molecular mechanism and mode of action of this protein remain elusive. cAMP-dependent protein kinase (PKA), along with other kinases, has been suggested to be an upstream kinase regulating LRRK2 function. Using MS, we detected several sites phosphorylated by PKA, including phosphorylation sites within the Ras of complex proteins (ROC) GTPase domain as well as some previously described sites (S910 and S935). We systematically mapped those sites within LRRK2 and investigated their functional consequences. S1444 in the ROC domain was confirmed as a target for PKA phosphorylation using ROC single-domain constructs and through site-directed mutagenesis. Phosphorylation at S1444 is strikingly reduced in the major PD-related LRRK2 mutations R1441C/G/H, which are part of a consensus PKA recognition site (^{1441}RASpS^{1444}). Furthermore, our work establishes S1444 as a PKA-regulated 14-3-3 docking site. Experiments of direct binding to the three 14-3-3 isotypes gamma, theta, and zeta with phosphopeptides encompassing pS910, pS935, or pS1444 demonstrated the highest affinities to phospho-S1444. Strikingly, 14-3-3 binding to phospho-S1444 decreased LRRK2 kinase activity in vitro. Moreover, substitution of S1444 by alanine or by introducing the mutations R1441C/G/H, abrogating PKA phosphorylation and 14-3-3 binding, resulted in increased LRRK2 kinase activity. In conclusion, these data clearly demonstrate that LRRK2 kinase activity is modulated by PKA-mediated binding of 14-3-3 to S1444 and suggest that 14-3-3 interaction with LRRK2 is hampered in R1441C/G/H-mediated PD pathogenesis.

cAMP-dependent protein kinase | protein–protein interaction | pathogenic mutation

Parkinson disease (PD), one of the most prevalent neurodegenerative afflictions, is characterized pathologically by the selective loss of dopaminergic neurons in the midbrain and by the presence of intracellular inclusions in the remaining cells, termed Lewy bodies (1). However, the molecular mechanisms underlying the complex pathological process are poorly understood. Many genetic and environmental factors contribute to the disease, and mutations in the leucine-rich repeat kinase 2 (LRRK2) gene are the most common cause of familial PD. LRRK2 is a large protein of 285 kDa and encodes several structural motifs, such as armadillo, ankyrin, and the namesake leucine-rich repeats, a Ras of complex proteins (ROC) GTPase, a C-terminal of ROC (COR), a kinase domain [with sequence homology to MAP kinase kinase kinase (MAPKKKs)], and a C-terminal WD40 domain (2). Notably, mutations known to cause PD are located within the catalytically active GTPase (ROC) and kinase domains of LRRK2 (see Fig. 3*A*) (3). Particularly for a single residue located within the ROC domain, three independent PD-associated mutations (R1441C, R1441G, and R1441H) have been found (4), whereas the kinase domain may harbor the most frequent pathogenic mutation, G2019S. Mutations at both these sites have been associated with enhanced kinase activity compared with wild type (5, 6), suggesting that dysregulation of these enzymatic activities may contribute to PD pathogenesis.

LRRK2 is a cytosolic phosphoprotein (7) phosphorylated in vitro by a variety of serine/threonine kinases, including PKC zeta (8), serine protein kinase ataxia telangiectasia mutated (9), the IκB kinase family (10), and cAMP-dependent protein kinase (PKA) (11, 12). PKA is a key regulator of a vast number of signaling molecules and is critical for neuronal functions such as synaptic plasticity, protein trafficking, protein degradation, neuronal excitability, and regulation of dopamine physiology (13–17). In LRKK2, the conserved residue (S935) was shown to be phosphorylated by PKA (12), and recently this site was proposed as a biomarker for LRRK2 activity (10, 18, 19). Phosphorylation of S910 and S935 within LRRK2 promotes binding of 14-3-3 proteins (19), a family of small 29–30 kDa acidic regulatory proteins, highly conserved and ubiquitously expressed in various tissues. The binding of 14-3-3 proteins results in various downstream effects, such as changes in structural conformations, kinase activity, and subcellular localization of the target proteins (20, 21). Nichols et al. (19) proposed a role for 14-3-3 proteins in regulating the cytoplasmic localization of LRRK2, whereas Li et al. (12) observed protection from dephosphorylation of S935 after 14-3-3

Significance

Leucine-rich repeat kinase 2 (LRRK2) is a multidomain protein implicated in Parkinson disease, and cAMP-dependent protein kinase (PKA) has been suggested to act as an upstream kinase phosphorylating LRRK2. Using a phosphoproteomics approach, we identified several novel PKA phosphorylation sites on LRRK2. We could demonstrate that one PKA phosphosite comprises the second most common mutation in LRRK2 (R1441C/G/H) attributed to Parkinson disease. Our findings reveal that this site is mandatory for subsequent 14-3-3 binding and affects LRRK2 kinase activity. These data provide a mechanistic insight into the regulation of LRRK2 kinase activity and its perturbation by disease-associated mutations.

Author contributions: K.M., D.B., M.U., C.J.G., and F.W.H. designed research; K.M., D.B., F.v.Z., and C.J.G. performed research; F.G., J.S.H., A.G., and A.J. contributed new reagents/analytic tools; K.M., D.B., and C.J.G. analyzed data; and K.M., D.B., C.J.G., and F.W.H. wrote the paper.

The authors declare no conflict of interest.

*This Direct Submission article had a prearranged editor.

[1]C.J.G. and F.W.H. contributed equally to this work.

[2]To whom correspondence should be addressed. E-mail: herberg@uni-kassel.de.

This article contains supporting information online at www.pnas.org/lookup/suppl/doi:10.1073/pnas.1312701111/-/DCSupplemental.

binding. Furthermore, recent data from Fraser et al. (22) suggest a regulatory function of 14-3-3 binding in controlling extracellular release of LRRK2. Dysregulation of 14-3-3/client protein interaction has been shown to facilitate the development of several human disorders (23, 24), and an influence of the pathogenic mutation R1441G on LRRK2/14-3-3 interaction has been demonstrated (12, 19). Although these data support an involvement of PKA and 14-3-3 proteins in regulating LRRK2 function, LRRK2 phosphorylation by PKA, as well as 14-3-3 binding and possible (patho)physiological consequences of this interplay, have not yet been addressed in detail.

Here, we systematically mapped PKA phosphorylation sites in LRRK2 and further investigated the impact of this phosphorylation in terms of 14-3-3 binding and LRRK2 function. Our results predict an essential function for PKA phosphorylation and subsequent 14-3-3 interaction in the negative regulation of LRRK2 kinase activity.

Results

Phosphosite Mapping by MS Reveals PKA Target Sites Within LRRK2. PKA previously was shown to phosphorylate S935 on LRKK2 (12). To systematically map other potential PKA phosphorylation sites within the LRRK2 sequence, we used MS. We performed in vitro kinase assays using purified kinase-dead (K1906M) full-length or kinase-dead N-terminal deletion (Δ967) mutants of LRRK2 expressed in insect cells as a substrate for purified catalytic (C)-subunit of human PKA. As a negative control for PKA specificity, experiments were performed in the presence of the heat-stable protein kinase inhibitor (PKI) (25). A total of 18 phosphorylated serine and 2 threonine residues were identified (Table S1), 15 of which correspond to residues already published (T833, S850, S858, S860, S908, S910, S933, S935, S954, S955, S958, S971, S973, S976, and S979), all of which are located between the ankyrin and LRR domain, which we previously termed constitutive phosphorylation cluster (7). Six serine residues (S910, S955, S971, S973, S976, and S979) also were found in the negative controls (Table S2), indicating that LRRK2 already was phosphorylated to some extent in the insect expression system. Remarkably, spectral counting showed that PKA treatment leads to an increase in identification of phosphopeptides, particularly peptides encompassing S910. Three of the identified phosphopeptides are located outside the constitutive phosphorylation cluster. One of these peptides resides in the ROC GTPase domain bearing the so-far uncharacterized residues pS1443 and pS1444 (Fig. S1), one peptide in the COR domain bearing T1849, and another peptide in the WD40 domain containing the phosphorylation site S2166 (Muda et al., in preparation). We focus our studies here on the analysis of S910, S1443, and S1444 that were recovered multiple times in MS-based approaches.

S910, Along with S935, Is a PKA Phosphorylation Site. S935 previously was described as a PKA phosphorylation site in vitro and in cell culture (12); furthermore, S910 and S935 were identified as putative IκB kinase sites (10). Here, we demonstrate that besides S935, S910 also is a PKA phosphorylation site. First, we phosphorylated recombinant LRRK2 WT (expressed and purified using Sf9 insect cells) with PKA in vitro and probed the samples with the phosphospecific antibody anti-pS910 or anti-pS935. LRRK2 already showed basal phosphorylation on both S910 and S935, which were increased significantly upon incubation with PKA (Fig. 1*A*). These in vitro findings were confirmed in cell culture with transfected COS7 cells after forskolin (FSK)/3-isobutyl-1-methylxanthine (IBMX) stimulation. Whereas FSK is a potent activator of adenylate cyclase, IBMX inhibits phosphodiesterase activity, causing a rapid increase of intracellular cAMP concentrations. Congruently, we observed an increase in LRRK2 phosphorylation at both S910 and S935 as a result of FSK/IBMX treatment compared with untreated controls (Fig. 1*B*).

PKA Phosphorylates the Isolated LRRK2 ROC Domain on S1443 and S1444. Because MS identified S1443 and S1444 as potential PKA phosphorylation sites (Table S1), isolated ROC GTPase domain (1334–1516) was used in an in vitro kinase assay. As shown in Fig. 2*A*, ROC WT was phosphorylated efficiently by PKA, and its phosphorylation was blocked in the presence of the PKA-specific inhibitor PKI. The ROC domain on its own did not incorporate any detectable radiolabel (Fig. 2*A*). These results were validated further by site-directed mutagenesis. ROC mutants were generated in which serines at position 1443, 1444 individually or together were substituted by alanine and incubated with PKA. Reaction products were visualized by autoradiography (Fig. 2*C*) or quantified in a scintillation counter (Fig. 2*D*). The S1443A mutant was as efficiently phosphorylated as the wild-type ROC domain (100%), whereas ^{32}P incorporation into S1444A was decreased significantly. The double mutant S1443A_S1444A resulted in a complete loss of the phosphorylation signal, suggesting that both residues may serve as PKA phosphorylation sites in LRRK2.

Mutation of a PKA Consensus Motif Largely Reduces Phosphate Incorporation at Both S1443 and S1444. An alignment of LRRK2 protein sequences from several mammalian species showed that S1443 and S1444, as well as their flanking motifs, are highly conserved (Fig. 2*B*). PKA, in particular, efficiently phosphorylates proteins containing the consensus sequence RRXpS/pT (where X is any amino acid and pS/pT is phosphorylated serine or threonine), but PKA-mediated phosphorylation does not depend strictly on this motif, and deviations in basic residues and spacing are tolerated, such as RXXpS/pT or RKXpS/pT and RXpS/pT, KRXpS/pT, or KKXpS/pT, found in confirmed in vivo substrates such as phosphorylase kinase, fructose-6-phosphate-1-kinase, fructose-1.6-bisphosphatase, and glycogen synthase (26–28). Interestingly, pS1444, together with the upstream residue R1441 (^{1441}**R**ASpS^{1444}) in LRRK2, constitutes an RXXpS/pT PKA recognition motif (26, 28), in which the third position preceding pS/pT should be occupied by an arginine (P-3, the corresponding position in LRRK2 is marked in bold and underlined) for PKA substrate recognition. Therefore, we hypothesized that the pathogenic mutation of arginine (on P-3) to a cysteine, glycine, or histidine residue would efficiently prevent phosphorylation by PKA. To answer this question, we probed the effect of the known pathogenic LRRK2 mutations R1441C/G/H within the ROC fragment on phosphorylation by PKA. Notably, neither ROC R1441C nor R1441G or R1441H were phosphorylated in an in vitro kinase assay by PKA (Fig. 2 *E* and *F*), identifying the arginine at position R1441 as a do-or-die situation for PKA phosphorylation at S1444.

PKA Phosphorylation of LRRK2 on S1444 Induces 14-3-3 Binding. Previous studies showed that phosphorylation of S910 and S935 promotes interaction of LRRK2 and 14-3-3 (12, 19). However, many 14-3-3 client proteins, such as Cdc25B, contain more than one 14-3-3 binding site (29). To examine the possibility that regions other than S910 and S935 might associate with 14-3-3, we performed GST–14-3-3 pull-down experiments with StrepII/Flag-tagged LRRK2 WT and a corresponding N-terminal truncation mutant (LRRK2 WT Δ967) lacking the 14-3-3 binding site around S910 and S935. GST–14-3-3 gamma showed specific interaction with wild-type and the N-terminally truncated LRRK2 compared with the GST control (Fig. 3*B*). Thus, LRRK2 WT Δ967, which does not contain S910/S935, was precipitated efficiently by GST–14-3-3 gamma, strongly indicating an additional 14-3-3 docking site in LRRK2.

Next, we looked at the residues that mediated 14-3-3 binding to LRRK2 WT Δ967 in detail. Most interactions between 14-3-3 proteins and their binding partners depend on phosphorylation of serine/threonine residues within discrete motifs in the target proteins, termed mode I (RSXpS/pTXP) and mode II [RX(F/Y)

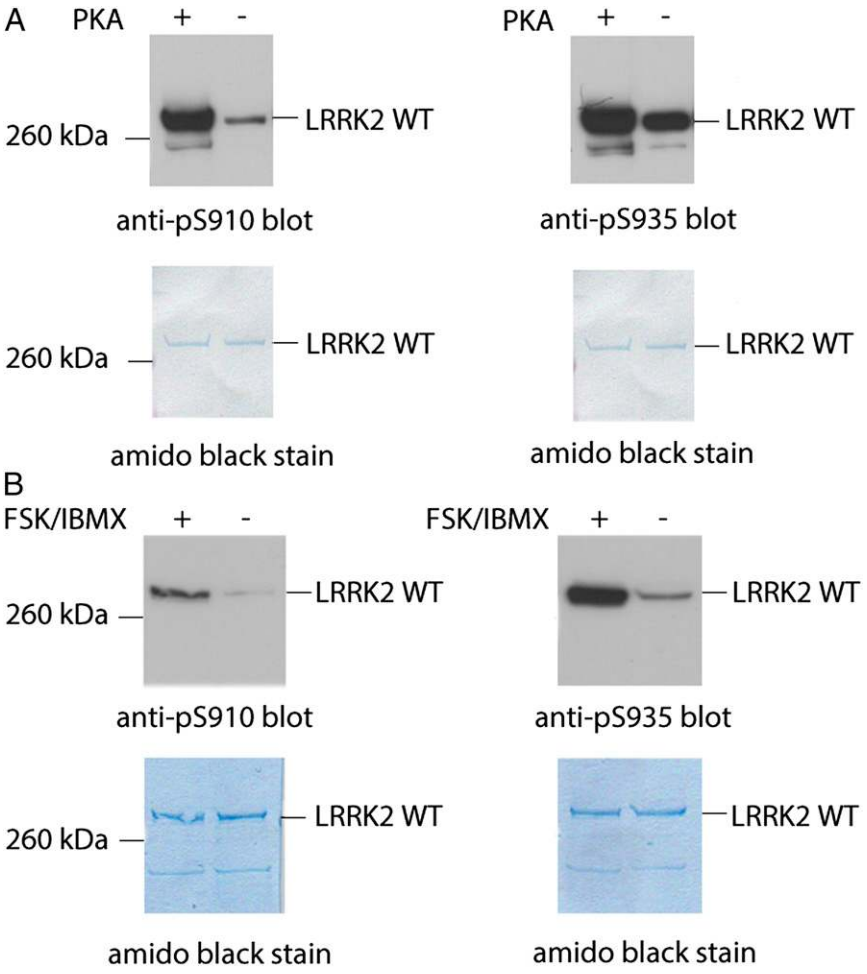

Fig. 1. S910 und S935 are both PKA phosphorylation sites in LRRK2. (*A*) StrepII/Flag-tagged LRRK2 WT purified from an insect cell expression system was phosphorylated by PKA in vitro. Products were separated on 4–12% gradient gels and analyzed by Western blot using phosphospecific antibodies against pS910 and pS935. (*B*) Forty-eight hours after transfection with StrepII/Flag-tagged LRRK2 WT, COS7 cells were serum starved for 4 h and subsequently incubated with 50 μM FSK and 100 μM IBMX for 30 min at 37 °C. LRRK2 subsequently was enriched with Strep-Tactin Superflow, separated by SDS/PAGE, and immunoblotted with anti-p910 or anti-p935 antibodies. Amido Black stain confirmed equal protein loading.

XpS/pTXP] (30). Interestingly, by comparing these motifs, we found that S1444, with its surrounding amino acid sequence, closely resembles a 14-3-3 mode I binding sequence (Fig. 3*A*).

To test whether S1444 has a potential role as a PKA-induced 14-3-3 binding site in LRRK2, we synthesized LRRK2 peptides containing nonphosphorylated S1444 (LFNIKARASSSPVILVGT) and phosphorylated S1444 (LFNIKARAS**pS**SPVILVGT) and examined their ability to compete with LRRK2 WT Δ967 binding to GST–14-3-3 gamma in a pull-down. By applying the peptides at increasing concentrations, we found that the peptide containing phosphorylated S1444 inhibited LRRK2 WT Δ967 interaction with GST–14-3-3 gamma in a dose-dependent manner, whereas no effect was observed for the corresponding nonphosphorylated peptide (Fig. 3*C*).

To test the hypothesis that PKA phosphorylation of LRRK2 region 1334–1516 (ROC GTPase domain, including S1444) might modulate its interaction with 14-3-3 proteins and to exclude other regions, we performed Far western assays with the isolated ROC domain. ROC WT was incubated in the presence or absence of PKA, and the proteins then were separated by SDS/PAGE and blotted to a PVDF membrane for Far western analysis (Fig. 3*D*). When recombinant 14-3-3 gamma was applied at a concentration of 0.1 μM, binding of 14-3-3 was detected exclusively to PKA-phosphorylated but not to nonphosphorylated ROC fusion protein. Beside the ROC WT, mutant proteins lacking the specific PKA phosphorylation sites (S1443A, S1444A, and S1443A_S1444A) were tested for 14-3-3 binding upon PKA treatment. Replacing serine 1444 by alanine completely abrogated the phosphorylation-dependent 14-3-3 interaction, whereas replacing the neighboring serine (S1443A) showed no significant reduction in 14-3-3 binding compared with ROC WT. Correspondingly, an ROC double-mutant S1443A_S1444A also showed no interaction with 14-3-3 after PKA incubation.

Determination of Binding Affinities of LRKK2 to 14-3-3. To further characterize the binding capability of LRRK2, posttranslationally modified at serine 1444, to 14-3-3, we analyzed 14-3-3 binding to either phosphorylated or nonphosphorylated LRRK2 peptides by fluorescence polarization (FP) and surface plasmon resonance (SPR). FP was used to determine the affinity of three 14-3-3 isoforms (gamma, theta, and zeta) to four different fluorescein-labeled LRRK2 peptides. Besides a peptide encompassing the LRRK2 residues R1441, S1443, and S1444 (referred to as wild-type sequence), three variant peptides, containing S1444 phosphorylation, the pathogenic mutation R1441G, or the nonphosphorylable variant S1444A, were tested. The peptides were incubated in the presence or absence of PKA and subsequently mixed with the respective 14-3-3 proteins before the FP signal was measured.

As shown in Fig. 4, phosphorylated LRRK2 WT peptide (pS-LRRK2-1444) bound to all three 14-3-3 isoforms, indicated by a high FP signal, whereas the nonphosphorylated WT LRRK2 peptide did not bind to any of the 14-3-3 isoforms. Preincubation of the nonphosphorylated WT peptide with recombinant PKA led to a significant increase in binding to all 14-3-3 isoforms. As a control, WT peptide phosphorylation was blocked in the presence of PKI (1 μM) during PKA preincubation, and subsequently no interaction with 14-3-3 protein was observed. The peptides

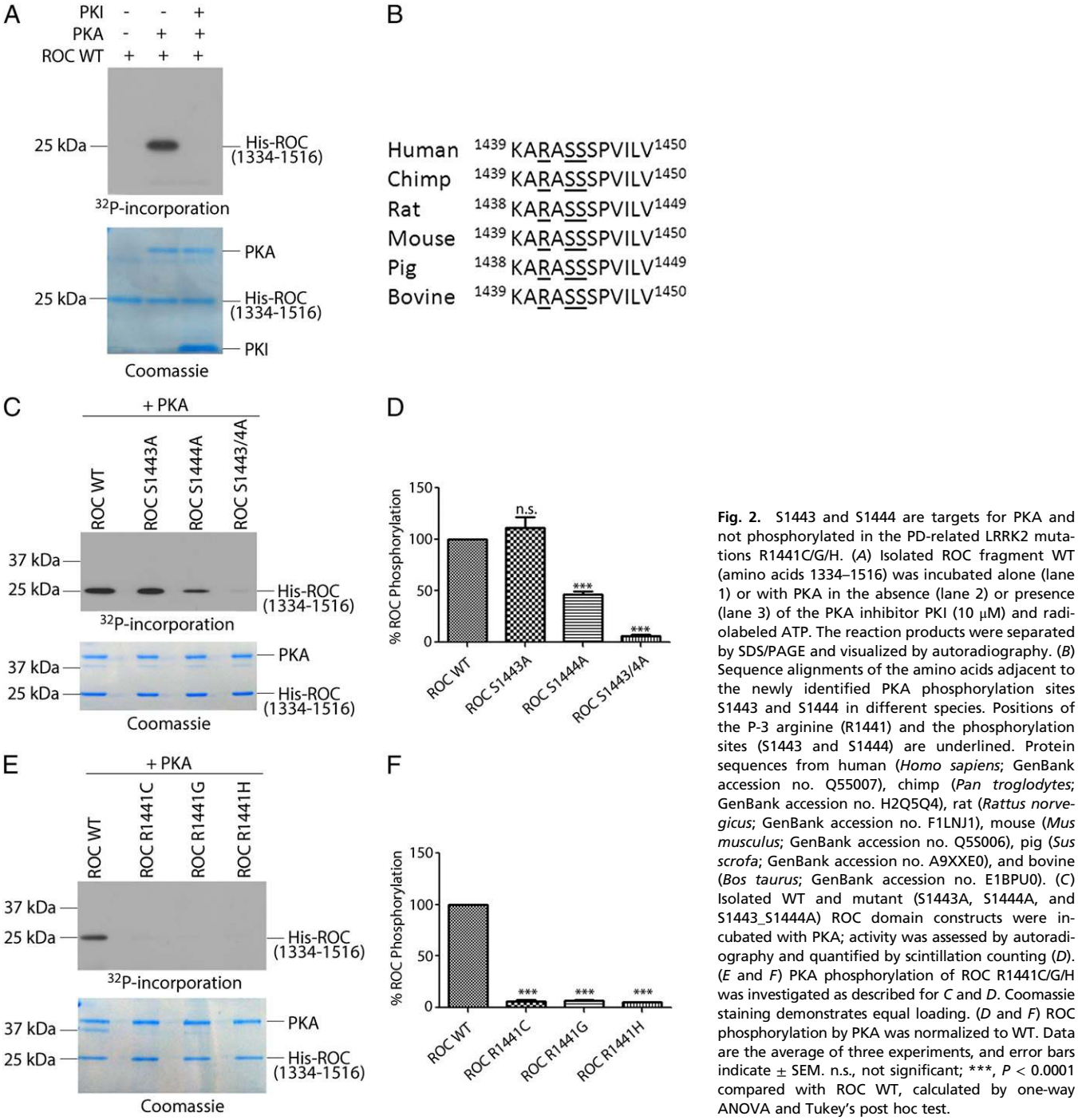

Fig. 2. S1443 and S1444 are targets for PKA and not phosphorylated in the PD-related LRRK2 mutations R1441C/G/H. (*A*) Isolated ROC fragment WT (amino acids 1334–1516) was incubated alone (lane 1) or with PKA in the absence (lane 2) or presence (lane 3) of the PKA inhibitor PKI (10 μM) and radiolabeled ATP. The reaction products were separated by SDS/PAGE and visualized by autoradiography. (*B*) Sequence alignments of the amino acids adjacent to the newly identified PKA phosphorylation sites S1443 and S1444 in different species. Positions of the P-3 arginine (R1441) and the phosphorylation sites (S1443 and S1444) are underlined. Protein sequences from human (*Homo sapiens*; GenBank accession no. Q55007), chimp (*Pan troglodytes*; GenBank accession no. H2Q5Q4), rat (*Rattus norvegicus*; GenBank accession no. F1LNJ1), mouse (*Mus musculus*; GenBank accession no. Q5S006), pig (*Sus scrofa*; GenBank accession no. A9XXE0), and bovine (*Bos taurus*; GenBank accession no. E1BPU0). (*C*) Isolated WT and mutant (S1443A, S1444A, and S1443_S1444A) ROC domain constructs were incubated with PKA; activity was assessed by autoradiography and quantified by scintillation counting (*D*). (*E* and *F*) PKA phosphorylation of ROC R1441C/G/H was investigated as described for *C* and *D*. Coomassie staining demonstrates equal loading. (*D* and *F*) ROC phosphorylation by PKA was normalized to WT. Data are the average of three experiments, and error bars indicate ± SEM. n.s., not significant; ***, $P < 0.0001$ compared with ROC WT, calculated by one-way ANOVA and Tukey's post hoc test.

containing either the pathogenic variant LRRK2-R1441G or the phospho-dead variant LRRK2-S1444A showed no interaction with any 14-3-3 protein, independent of PKA pretreatment (Fig. 4).

Next, we measured the affinity of the two corresponding peptides to each 14-3-3 isoform in a direct FP-binding assay using 10 nM of fluorescein-labeled peptide each and a serial dilution of the corresponding 14-3-3 protein. Phosphorylated WT peptide (pS-LRRK2-1444) bound to 14-3-3 gamma with an affinity of 220 nM, whereas the nonphosphorylated WT peptide showed no binding (Fig. S2). The affinity for 14-3-3 theta (K_d: 940 nM) and 14-3-3 zeta (K_d: 650 nM) was determined to be 4.5-fold and 3.3-fold lower, respectively (Table 1).

Using FP, we further quantitatively compared 14-3-3 binding to phospho-S1444 with the recently published phosphorylation sites S910 and S935. Phosphorylated and nonphosphorylated peptides were synthesized corresponding to phospho-S910 (pS-LRRK2-910, SFLVKKKSN**pS**ISVGEFYRD) or phospho-S935 (pS-LRRK2-935, SPNLQRHSN**pS**LGPIFDHED). Based on those experiments, the phosphopeptide pS-LRRK2-1444 corresponding to the ROC domain had higher affinities for 14-3-3 gamma, theta, and zeta compared with pS-LRRK2-910 (Table 1). None of the corresponding nonphosphorylated peptides showed binding to 14-3-3 proteins (Table 1 or Fig. S2). It is noteworthy that in contrast to previous reports describing phosphorylated

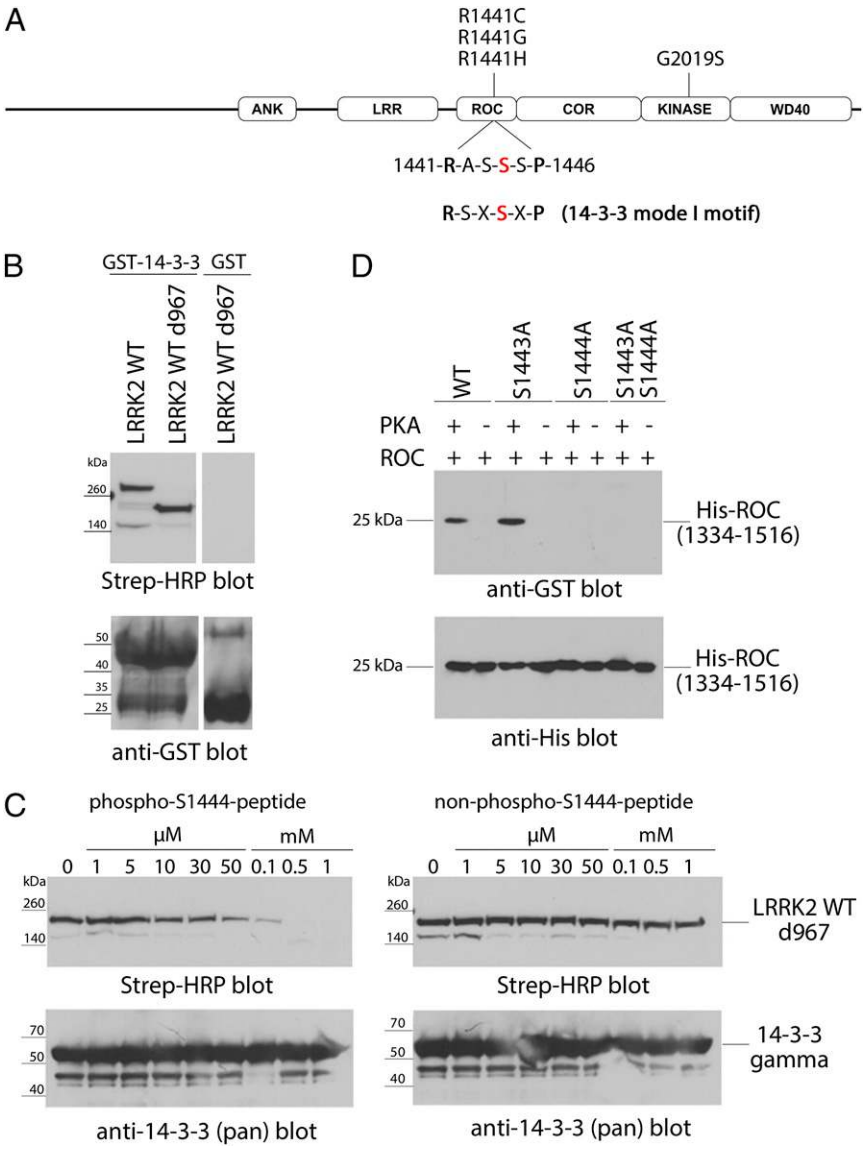

Fig. 3. S1444 on LRRK2 is a PKA-induced 14-3-3 binding site. (*A*) Multidomain structure of LRRK2. ANK, ankyrin repeat region; LRR, leucine-rich repeat domain; ROC, Ras of complex (GTPase); COR, C-terminal of ROC. The potential 14-3-3 interaction motif in LRRK2 is shown and aligned to a mode I 14-3-3 binding consensus sequence. Known pathogenic mutations R1441C/G/H and G2019S are indicated. (*B*) LRRK2 pull-down with recombinant GST–14-3-3 gamma. LRRK2 WT and LRRK2 WT Δ967 were expressed in Sf9 cells. Lysates were incubated with GST–14-3-3 gamma for 4 h. GST–14-3-3 gamma pulled down both LRRK2 WT full length and LRRK2 WT Δ967. Samples were separated on a 4–12% gradient SDS gel, and the membranes were probed with Strep-Tactin HRP or GST antibody. (*C*) LRRK2 WT Δ967 was precipitated with GST–14-3-3-agarose in the absence or in the presence of increasing concentrations of chemically synthesized LRRK2 peptides (LFNIKAR-ASSSPVILVGT) phosphorylated or nonphosphorylated at S1444. Sample separation and Western blotting were carried out as described under **B**. (*D*) Two micrograms of His-ROC WT, S1443A, S1444A, or S1443A-S1444A mutant proteins was incubated in the presence or absence of PKA for 1 h at 30 °C. Far western blotting was performed using GST–14-3-3 protein as a probe. PKA-induced ROC–GST–14-3-3 interaction could be observed only when S1444 was present. Equal loading was demonstrated using anti-His antibody.

S935 as a 14-3-3 acceptor site (12, 19), we found no significant binding of the pS-LRRK2-935 phosphopeptide to 14-3-3.

We also applied SPR for direct interaction analysis between N-terminally biotinylated, unphosphorylated (S1444) and phosphorylated (pS1444) LRRK2 peptides immobilized separately on one sensor chip, and injected 14-3-3 protein gamma, theta, or zeta over the surface. None of the three isoforms interacted with the unphosphorylated peptide, whereas binding to the phosphorylated peptide was clearly detectable (Fig. 5). Taken together, the above experiments suggest that LRRK2 phosphorylated at S1444 directly binds to 14-3-3 and that this interaction depends on phosphorylation by PKA.

Phosphorylation of S1444 Modulates LRRK2 Kinase Activity. To investigate a possible regulatory function of 14-3-3 binding on LRRK2 activity, we compared the kinase activity of recombinant LRRK2 WT with that of the LRRK2 variants S1444A and R1441H. As a control for enhanced LRRK2 activity, we monitored LRRK2 kinase activity of the disease-associated mutation G2019S, characterized by increased kinase activity (6, 31). Using an in vitro kinase assay in the presence of [^{32}P]ATP, LRRK2 activity was determined by measuring LRRK2 autophosphorylation as well as by using GST–moesin as a substrate (Fig. 6*A*) (32). In both cases, when either the PKA phosphorylation site S1444 or the P-3 arginine 1441 of the PKA consensus motif was mutated, a slight increase in LRRK2 kinase activity was observed. Although the increase in autophosphorylation activity for LRRK2 R1441G and S1444A clearly was lower than for LRRK2 G2019S, all three variants phosphorylated GST–moesin equally well, possibly indicating complete GST–moesin phosphorylation (Fig. 6). As shown in Fig. 6*B*, autophosphorylation of LRRK2 was increased 1.6-fold in LRRK2 R1441H and S1444A compared with LRRK2 WT, as determined by liquid scintillation counting. For LRRK2 G2019S, we observed enhanced protein autophosphorylation activity of approximately threefold, as described earlier by others (19, 33). To exclude that the observed increase in activity was caused by the amino acid substitution itself rather than by PKA-mediated phosphorylation and to test whether LRRK2 kinase activity is regulated by 14-3-3 binding on S1444 in vitro, we performed kinase assays monitoring phosphorylation of the previously identified LRRK2 autophosphorylation site T2483 (7) in the presence or absence of PKA, 14-3-3, or both (Fig. 6*C*). We could demonstrate that this site is not phosphorylated by PKA in vitro (Fig. S3*A*), making this site suitable to selectively determine LRRK2 autokinase activity in

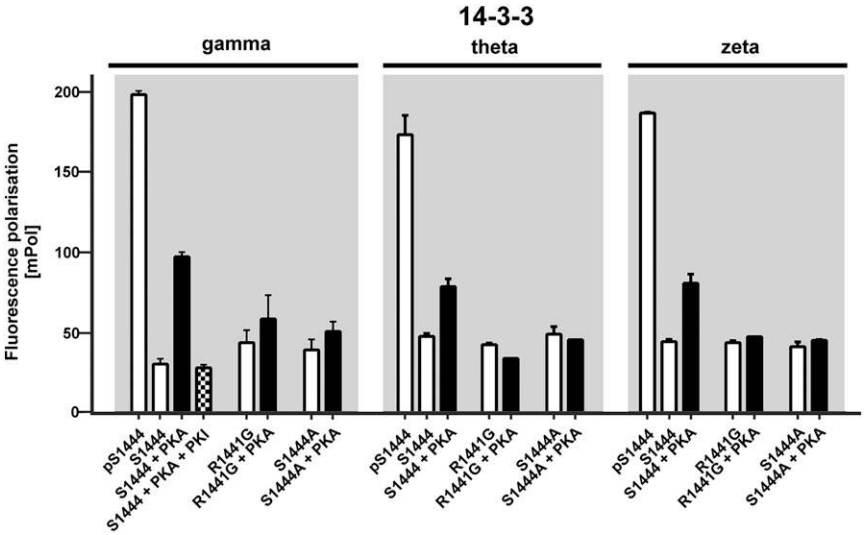

Fig. 4. Binding of GST–14-3-3 to synthetic peptides corresponding to the newly identified 14-3-3 binding region of LRRK2. Direct FP assays: 20 nM of fluorescein-labeled LRRK2 peptides were incubated in the presence or absence of 500 nM PKA in kinase buffer. Control experiments were performed in the presence of the PKA-specific inhibitor PKI (10 μM). Each data point represents the mean ± SEM from triplicate measurements.

the presence of active PKA (Fig. 6*C*). LRRK2 WT, R1441H or S1444A, PKA, or 14-3-3 gamma alone had no effect; however, the combination of PKA and 14-3-3 gamma caused a decrease in LRRK2 autokinase activity. In line with these findings, inhibition was blocked in the presence of the PKA-specific inhibitor protein PKI (Fig. S3*B*). Notably, whereas the kinase activity of LRRK2 WT was decreased in the presence of PKA and 14-3-3 gamma, LRRK2 R1441H and S1444A showed no effect on kinase activity (Fig. 6*C*).

Discussion

Several mutations in LRRK2 have been linked to PD, yet molecular mechanisms contributing to this disease remain largely undefined. Several lines of evidence implicate that altered kinase activity of LRRK2 may play an important role in neurodegeneration (34, 35). In addition, LRRK2 is a phosphoprotein, being phosphorylated at various sites via either autophosphorylation or upstream kinases (7, 18). Here, we extend current knowledge demonstrating that PKA-mediated phosphorylation of LRRK2 can modulate LRRK2 kinase activity and control 14-3-3 binding, thus correlating PD-related mutations with a disturbed phosphorylation pattern.

PKA also is one of the key regulators in signal transduction in the brain. This kinase is activated in response to increasing concentrations of cAMP and phosphorylates a vast number of protein kinases, including the MAPKKK c-Raf (36). Furthermore, PKA facilitates synaptic transmission (13) and assumes an important function as a regulator of dopamine synthesis (17). In this context, the occurrence of the recently published PKA phosphorylation site S935 in LRRK2 (12) implicates a possible involvement of PKA in regulating LRRK2 function. Here, we examine the functional relevance of PKA phosphorylation in LRRK2 and provide evidence for PKA acting as an upstream kinase for LRRK2. Based on the PKA consensus substrate motifs RRXpS/pT, RXXpS/pT, and KKXpS/pT described by Kemp et al. (26), in silico sequence analysis predicted several putative PKA phosphorylation sites within LRRK2. We experimentally identified 20 serine/threonine residues being phosphorylated within LRRK2 after PKA treatment. In agreement with a previous report (12), our study demonstrates that PKA can phosphorylate LRRK2 at S935 in vitro as well as in cell culture. Furthermore, we could demonstrate that phosphorylation at S910 is increased either upon PKA treatment in vitro or by FSK/IBMX stimulation in cell culture.

In addition to S910, we identified PKA-mediated phosphorylation of the phosphoacceptor sites S1443 and S1444, previously reported by Pungaliya et al. (37). These sites are located within the LRRK2 GTPase domain ROC already described as a target for autophosphorylation (7). Using the recombinant ROC domain, we could verify the residues S1443 and S1444 as PKA substrate sites, in vitro. However, we cannot exclude that other kinases, such as protein kinase B (Akt/PKB), phosphorylate these two sites. The consensus motif of Akt/PKB (K/RxK/RxxS/T) also matches the sequence around S1444. However, as demonstrated by Ohta et al. (38), Akt/PKB acts as an LRRK2 substrate rather than an LRRK2 upstream kinase. Interestingly, the residues S1443 and S1444 are located close to the PD-causing mutations R1441C/G/H (4). These mutations critically alter the general PKA consensus motif RXXS formed by the residues 1441–1444. Indeed, we could confirm that the PD mutation R1441G completely abolishes PKA phosphorylation at the sites S1443 and S1444, giving unique mechanistic insights into the pathogenesis of LRRK2 mutations.

Nichols et al. (19) and Li et al. (12) recently identified 14-3-3 proteins as binding partners of LRRK2 interacting with residues pS910 and pS935 localized between the ankyrin and LRR domains. Here, we demonstrate the presence of additional 14-3-3 sites based on GST pull-down experiments with an N-terminally truncated version of LRRK2 (Δ967) not containing S910 and S935. Interestingly, our newly identified PKA phosphorylation site (^{1441}RAS**pS**SP^{1446}) resembles a canonical 14-3-3 binding motif type I as described by Yaffe et al. (30) (RSXpSXP or RXXXpSXP). Consequently, we show that 14-3-3 specifically binds only the PKA-phosphorylated ROC domain or LRRK2 peptides

Table 1. Binding constants for the fluorescein-labeled synthetic peptides corresponding to pS910, pS935, and the newly identified 14-3-3 binding region of LRRK2 containing pS1444 to three different 14-3-3 isoforms derived from FP measurements

	K_d (nM) ± SD		
Peptide	14-3-3 gamma	14-3-3 theta	14-3-3 zeta
pS910	661 ± 121	4,100 ± 416	1,336 ± 318
pS935	—	—	—
pS1444	216 ± 44	938 ± 85	653 ± 93

K_d determinations were carried out as detailed in the Fig. S2 legend. K_d values were derived from seven independent experiments (three protein preparations), each performed in triplicate.

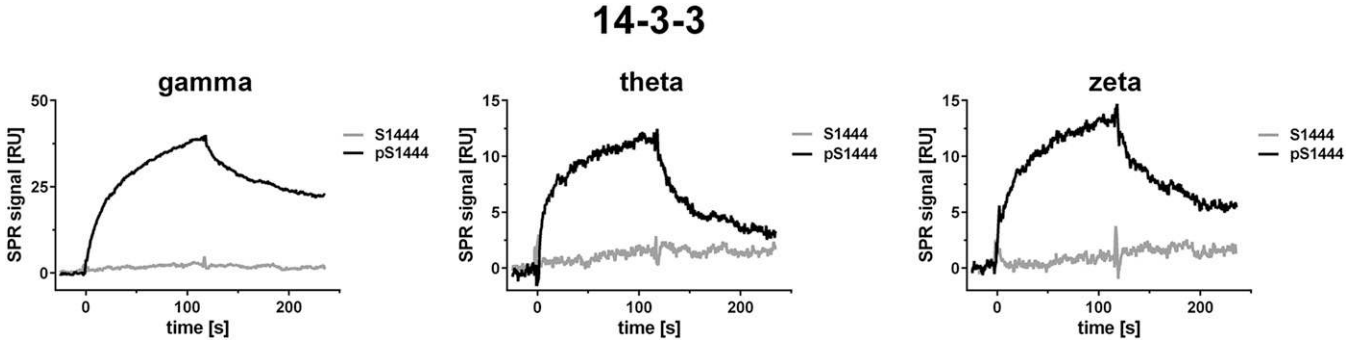

Fig. 5. SPR analysis of the interaction of GST–14-3-3 with synthetic peptides corresponding to the newly identified 14-3-3 binding region of LRRK2 S1444. Sixty nanomolars of S1444 peptides, either unphosphorylated (S1444, gray line) or phosphorylated (pS1444, black line) was immobilized via a biotin linker to the sensor surface, and 14-3-3 (gamma, theta, or zeta, 1 μM each) was injected over the surface. Only the phosphorylated peptide shows binding to the different 14-3-3 proteins. The maximum SPR signal of 14-3-3 theta and zeta is reduced in comparison with the gamma isoform, indicating a lower affinity to pS1444.

containing the sequence motif ^{1441}RAS**pS**SP^{1446}. Intriguingly, we could demonstrate that the PD-associated mutations at R1441C/G/H or mutations at S1444 abolish complex formation with the 14-3-3 isoforms gamma, theta, and zeta.

In mammals, seven 14-3-3 isoforms exist, forming homo- as well as heterodimers. Generally, 14-3-3–interacting proteins show a distinct preference for a specific 14-3-3 isoform. For instance, whereas tryptophan hydroxylase binds to all 14-3-3 isoforms, the MAPKKK c-Raf preferentially interacts with the beta and zeta isoforms (39, 40). In our study, we analyzed 14-3-3 gamma, theta, and zeta for their binding to LRRK2, as these isoforms previously were shown to bind LRRK2 (12, 19) and are present within Lewy bodies (23, 41). Based on FP and SPR, we provide evidence that all three 14-3-3 isoforms interact with LRRK2 peptides containing S1444 in a phosphorylation-dependent manner. Among the isoforms tested, 14-3-3 gamma shows the highest affinity for LRRK2. With a K_d of about 210 nM, the affinity of 14-3-3 gamma is similar to that of other 14-3-3 client proteins with K_d values ranging between 55 and 190 nM (30, 42). Furthermore, our findings are consistent with results by Li et al. (12) that also suggest a preferential LRRK2 association with 14-3-3 gamma.

When we quantified 14-3-3 binding to pS1444 in comparison with binding to pS910 and pS935, only peptides containing pS910 and pS1444 could bind 14-3-3, whereas pS935, previously proposed as a major 14-3-3 client site of LRRK2, did not show significant binding to any of the 14-3-3 isoforms tested. One explanation for this unexpected finding is that previous studies were based on longer, diphosphorylated peptides containing both pS910 and p935 (19) and thus not capable of differentiating between these sites. Comparing the K_d values of 14-3-3 binding to pS910 and to pS1444 reveals a two- to fourfold higher affinity of 14-3-3 to the newly identified PKA site pS1444. This may be explained by the sequence surrounding of S910 not matching a perfect 14-3-3 consensus binding motif. We conclude that LRRK2 contains at least two distinct binding regions for 14-3-3; one is located within the N-terminus encompassing the region around pS910 (19), and another, higher-affinity site is located in the ROC domain encompassing pS1444. Multiple binding sites as a requirement for stable 14-3-3 association have been demonstrated for Cdc25B (29) and c-Raf (43). Because 14-3-3 proteins form dimers, an LRRK2 molecule might associate with one 14-3-3 monomer via the pS910 motif and the other 14-3-3 monomer interacting with the newly identified pS1444 motif located within the ROC domain (see also Fig. 7).

Dysregulation of 14-3-3/target protein interaction has been associated with several human disorders, including PD, establishing 14-3-3 proteins as a novel class of molecules for therapeutic intervention (44). In agreement with the findings by Li et al. (12) and Nichols et al. (19), we demonstrate that 14-3-3 binding is impaired in the common familiar LRRK2 mutation R1441C/G/H. However, the latter reports correlate reduced phosphorylation of S910 and S935 in the pathogenic LRRK2 R1441G protein with a perturbed 14-3-3/LRRK2 interaction. Our results give a unique mechanistic explanation of how a mutation of an arginine in the P-3 position to a cysteine, glycine, or histidine prevents phosphorylation by PKA and thus efficiently

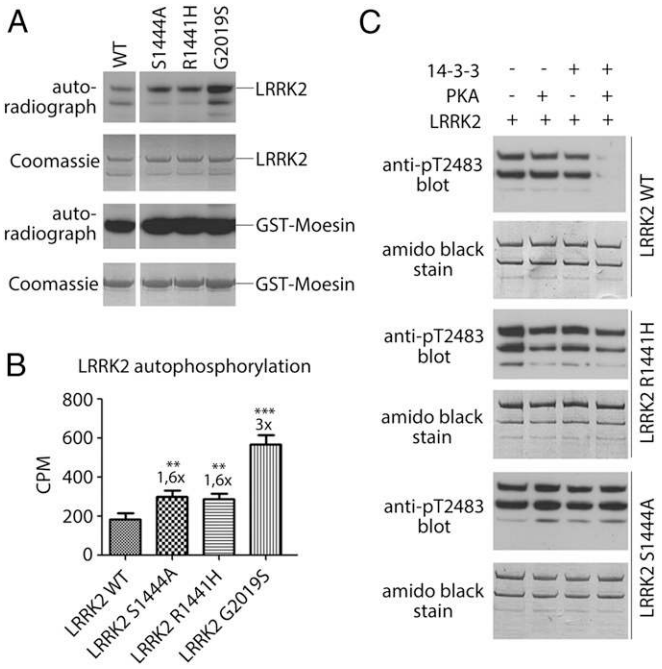

Fig. 6. LRRK2 kinase activity is modulated by phosphorylation of S1444 and 14-3-3 binding. (*A*) Activity of LRRK2 WT, S1444A, R1441H, and G2019S was determined in a radioactive in vitro kinase assay using GST–moesin as substrate. Probes were visualized by autoradiography. Samples were analyzed on the same gel, and equal protein loading was confirmed via Coomassie staining. (*B*) Incorporation of ^{32}P into LRRK2 protein bands was measured by liquid scintillation. Error bars represent ± SEM, and results from three independent experiments are shown (one-way ANOVA and Tukey's post hoc test). **, $P < 0.001$; ***, $P < 0.0001$ relative to LRRK2 WT. (*C*) Kinase activity of LRRK2 WT, R14441H, and S1444A also was measured by LRRK2 autophosphorylation in the presence of PKA and/or GST–14-3-3 gamma in vitro. Immunoblotting was performed with anti-pT2483 antibody, and equal protein loading was warranted by Amido Black staining.

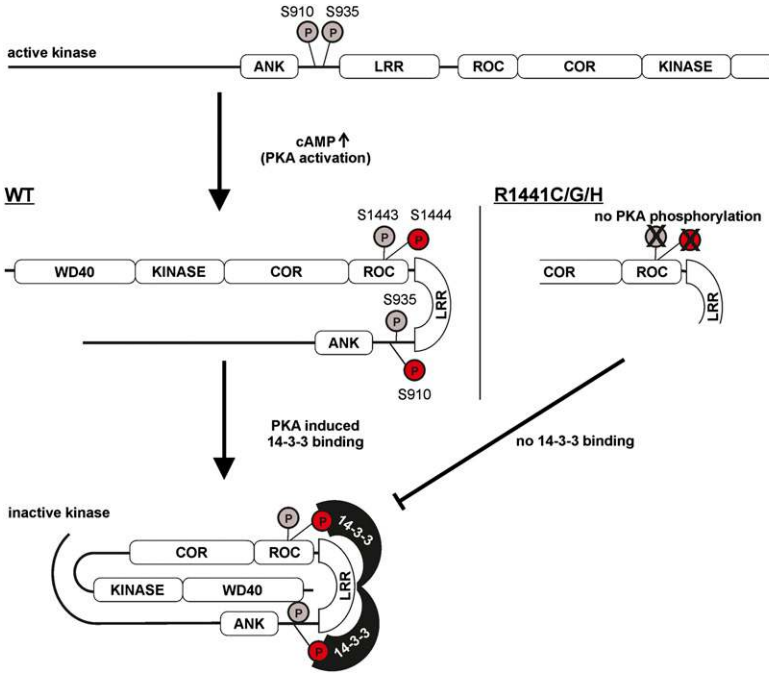

Fig. 7. Model for the regulation of LRRK2 kinase activity via PKA-mediated 14-3-3 binding to the ROC GTPase domain. Based on the experimental data, we propose a model in which LRRK2 kinase activity is controlled by a conformational change driving the kinase into an inactive state, which is stabilized by 14-3-3 interaction with pS910 and pS1444 (marked in red). Phosphorylation of S910 and S1444 in the ROC GTPase domain is mediated by the catalytic subunit of PKA. S1444 phosphorylation is abrogated in the PD-related LRRK2 mutations of R1441, thus preventing PKA-mediated attenuation of LRRK2 kinase activity.

impairs the interaction of LRRK2 with 14-3-3 proteins. An alternative concept recently was presented by Daniëls et al. (45), who correlate the R1441G mutation with weakened ROC–COR interdomain interaction, which in turn affects GTPase activity shown to negatively regulate LRRK2 kinase activity.

The 14-3-3 proteins dynamically control the activity of many intracellular proteins that regulate different physiological and pathophysiological processes (41). Our data suggest that LRRK2–14-3-3 interaction might control kinase activity, as mutations at R1441 or S1444 do influence LRRK2 catalytic activity. In particular, we have shown that the LRRK2 mutants R1441H and S1444A, both of which prevent 14-3-3 binding to the ROC domain, had an ~1.6 times enhanced LRRK2 kinase activity. This finding is in agreement with other studies in which enhanced kinase activity already was correlated with the PD-linked LRRK2 mutation R1441C (5, 9). On the other hand, LRRK2 WT kinase activity is decreased in the presence of 14-3-3 and PKA in vitro, whereas LRRK2 S1444A (P-site) or R1441H (P-3 site) are unaffected. Binding of 14-3-3 is thought to play an important role in modulating kinase activity, such as c-Raf and Bad, by stabilizing specific conformations, leading to either their inhibition or activation (46, 47).

Our results explain how the lack of negative feedback regulation by upstream kinases might contribute to the pathophysiology underlying R1441C/G/H mutations. Taken together, 14-3-3 may regulate LRRK2 kinase activity negatively by stabilizing an inactive conformation of LRRK2 (Fig. 7). In particular, phosphorylation of S1444 allows PKA in combination with 14-3-3 to delicately counterbalance LRRK2 activity, mediating an overall negative regulation on LRRK2 kinase activity. This idea is supported further by the fact that the newly identified 14-3-3 binding motif in LRRK2 is conserved between different species. Interestingly, it was proposed previously that the GTP-bound state of a subgroup of GTPases, including Roco proteins, may induce juxtaposition of two GTPase domains in a homodimer (48). In agreement with this model, PKA phosphorylation and subsequent binding of 14-3-3 might regulate LRRK2 kinase activity negatively by preventing dimerization of its ROC domain. Considering the recent findings by Daniëls et al. (45), this negative regulation also might be mediated by 14-3-3, affecting the interaction of ROC with the adjacent COR domain. Future studies are needed to correlate PKA-mediated phosphorylation of pS1444 with 14-3-3 binding and LRRK2 activity in vivo.

The regulative effects of PKA phosphorylation and 14-3-3 binding, described here, may foster concepts for the development of specific drugs targeting pathophysiological LRRK2 activity by allosteric effectors as a promising alternative to kinase inhibition by ATP-competitive compounds.

Materials and Methods

Generation of Fusion Proteins and Site-Directed Mutagenesis. The full-length human LRRK2 gene was generated as described in detail in Gloeckner et al. (49). For expression in insect cell culture, LRRK2 with a C-terminal tandem StrepII/Flag tag (50) was cloned into pFastBac1 (Invitrogen). According to the manufacturer's instructions, LRRK2 baculovirus was produced with the Bac-to-Bac expression system (Invitrogen). Adherent Sf9 insect cells were infected with virus with a multiplicity of infection of 10 and harvested after 72 h. Cells then were lysed in lysis buffer [100 mM Tris (pH 7.4), 130 mM NaCl, 1 mM NaF, 1% Triton X-100, all from Roth] supplemented with protease inhibitor mixture (cOmplete EDTA-free; Roche) and DNase I (80 U/μL; Applichem) at 4 °C for 30 min and centrifuged at 16,000 × *g* for 10 min. Supernatant including solubilized proteins was used for Strep-Tactin Superflow affinity chromatography following the supplier's instructions (IBA GmbH). Purified protein was stored in elution buffer [100 mM Tris (pH 8.0), 150 mM NaCl, 1 mM EDTA, 2.5 mM desthiobiotin] containing 10% (vol/vol) glycerol, 0.1 mM EGTA, and 1 mM DTT at −80 °C.

A codon-optimized construct of isolated ROC domain was cloned into the hexahistidine-tagged fusion protein vector pETM-11 (EMBL) via NcoI/KpnI digestion. His_6-tagged human ROC (WT and mutants) was expressed overnight at room temperature in *Escherichia coli* BL21 (DE3) RIL cells (Novagen) after 400 μM isopropyl β-D-1-thiogalactopyranoside (IPTG) induction and purified using HIS-Select Cobalt Affinity resin (Sigma–Aldrich) and standard conditions. Proteins were stored in 20 mM Hepes (pH 7.4), 150 mM NaCl on ice.

Site-directed mutations were carried out using the QuikChange site-directed mutagenesis kit (Stratagene) according to the manufacturer's protocols.

The 14-3-3 theta and zeta genes used in the present study were amplified from human fetal brain from Matchmaker cDNA Library (Clontech) using standard PCR methods with High Fidelity PCR Enzyme Mix (Thermo Scientific). The resulting PCR products were cloned into bacterial pGex expression vector as EcoRI-SalI fragments. The pGex–14-3-3 gamma plasmid was a gift from Michael Yaffe, David H. Koch Institute for Integrative Cancer Research, Cambridge, MA (Addgene plasmid ID 13280) (51). GST–14-3-3 isoforms were expressed in *E. coli* BL21 (DE3) RIL cells (Novagen) with 100 μM IPTG induction

at room temperature for 4 h and purified using Glutathione Agarose 4B beads (Macherey–Nagel) according to the manufacturer's protocols.

Protein concentrations were assessed by the Bradford method with BSA as the standard or using SDS/PAGE followed by Coomassie staining.

Cell Culture and Stimulation of PKA *in Cellulo*. COS7 cells were maintained in DMEM with 10% (vol/vol) FCS (GE Healthcare) at 37 °C and 5% CO_2 atmosphere. Sf9 cell culture monolayer was maintained in Insect-XPRESS medium (Lonza) supplemented with 10% (vol/vol) FCS (GE Healthcare) in a 27 °C constant temperature incubator.

Before treatment with 50 μM FSK (Sigma–Aldrich) and 100 μM IBMX (Sigma–Aldrich), cells were serum starved in serum-free medium for 4 h. Subsequently, the cells were incubated for 30 min with these drugs. LRRK2 protein had to be enriched by Strep-Tactin Superflow (IBA). COS7 cells were washed once with 1X PBS and lysed in ice-cold lysis buffer [30 mM Tris (pH 7.4), 150 mM NaCl, 0.05% Nonidet P-40] supplemented with protease and phosphatase inhibitor mixture (Roche). Samples from Sf9 insect cells were prepared as described above. Supernatant including solubilized proteins was applied with suspended resin to Mobicol columns (MoBiTec). After being washed three times with washing buffer [100 mM Tris (pH 8), 150 mM NaCl, 1 mM EDTA], protein-bound resins were resuspended in 30 μL 4X NuPAGE sample buffer (Invitrogen) containing 0.25 mM DTT (Roth) and bound proteins were eluted by boiling at 95 °C for 5 min. Proteins were resolved by SDS/PAGE followed by transfer onto PVDF membrane (Roth). Phosphorylation of LRRK2 in PBS or FSK/IBMX-treated cells was detected by immunoblotting with the phosphospecific LRRK2 antibodies anti-pS910 and anti-pS935 (Biomol). Both antibodies were applied at a dilution of 1/10,000 overnight at 4 °C in 20 mM Tris (pH7.5), 140 mM NaCl, 0.05% Tween 20 (TBS-T) with 5% (wt/vol) milk powder. Immune complexes were visualized using anti-rabbit HRP secondary antibodies (GE Healthcare) and ECL chemiluminescence (PerkinElmer).

PKA Assay and Far Western Blot. His-tagged ROC domain constructs were tested as in vitro substrates for PKA. Equal amounts (~1 μg each) of purified proteins were incubated in either the absence or presence of the human catalytic subunit of PKA (Calpha1) (0.5 U/μL) or 10 μM of the pseudosubstrate PKA inhibitor PKI alpha (52) in kinase assay buffer [25 mM Tris·HCl (pH 7.5), 10 mM $MgCl_2$, 2 mM DTT, 0.1 mM Na_3VO_4, 5 mM β-glycerophosphate, and 0.1 mM ATP] comprising 2 μCi [γ-^{32} P]-ATP for 1 h at 30 °C under continuous agitation. Assays were set up in a total volume of 20 μL. Reactions were terminated by boiling with 10 μL of 4X NuPAGE sample buffer (Invitrogen) containing 0.25 mM DTT (Roth) for 2 min at 95 °C. Subsequently, products were separated on 4–12% gradient gels (Invitrogen); gels were stained with Coomassie Brilliant Blue, dried, and exposed to X-ray film. Gel slices containing isolated ROC domain were cut out and transferred into a scintillation counter, and the percentage of phosphate incorporation in ROC was calculated. All experiments were conducted at least three times. To compare levels of ^{32}P-incorporation, statistical significance was determined by performing a one-way ANOVA and Tukey's post hoc test using GraphPad Prism Version 5.0 (GraphPad Software).

Alternatively, PKA phosphorylation within LRRK2 was examined either by MS or by immunoblotting. For mapping phosphorylation sites within LRRK2 by MS, 400 nM purified LRRK2 protein was incubated with 40 nM PKA for 1 h at 30 °C.

For Far western analysis, 2 μg of isolated ROC domain was phosphorylated as described above. Reaction products were separated by SDS/PAGE and transferred onto PVDF membrane. The membrane was blocked in 5% (wt/vol) milk powder in TBS-T at room temperature for 1 h. Afterward, 0.1 μM GST–14-3-3 gamma was incubated with the membrane at 4 °C overnight, followed by washing with TBS-T and incubation with anti-GST antibody (GenScript) at a dilution of 1/3,000 for 1 h at room temperature in TBS-T with 3% (wt/vol) milk powder. To visualize the bands, HRP-conjugated secondary antibody and ECL chemiluminescence (PerkinElmer) were used. To ensure equal protein loading, the membrane was stripped in stripping buffer [25 mM glycin (pH 2.2), 1% SDS] at 60 °C for 15 min and probed with anti-His antibody (GE Healthcare) at a dilution of 1/40,000 for 1 h at room temperature in TBS-T with 5% (wt/vol) milk powder.

LRRK2 Kinase Assays. To determine LRRK2 kinase activity, radioactive and nonradioactive kinase assays were performed. GST–moesin (500 ng, kindly provided by Frank Gillardon, Boehringer Ingelheim, Biberach an der Riss, Germany) was denatured at 65 °C for 10 min and used as a substrate for purified LRRK2 (1 μg). The radioactive kinase reactions were carried out by incubating both proteins in kinase buffer for 1 h at 30 °C. Reaction products were visualized by autoradiography or quantified as described above. In a nonradioactive kinase assay, 1 μg of recombinant LRRK2 was incubated in kinase buffer with 10 μg GST–14-3-3 gamma and/or 9 U PKA for 1 h at 30 °C. The reaction was terminated by boiling at 95 °C for 2 min. LRRK2 activity was detected by Western blotting with anti-pT2483 antibody (Abcam) diluted to 1/2,000 in 5% (wt/vol) milk powder overnight at 4 °C. Subsequently, blot membranes were stained with Amido Black.

GST Pull-Down Assay and Competition of Precipitates by Peptides. Equal molar amounts of GST or GST–14-3-3 fusion proteins were conjugated to Glutathione Agarose 4B beads (Macherey–Nagel) according to supplier protocols. Then, 40 μL aliquots of conjugated agarose bead slurry were incubated with 1 mg of Sf9 cell lysate supernatant for 4 h in lysis buffer [30 mM Tris (pH 7.4), 150 mM NaCl, 0.5% Nonidet P-40] at 4 °C. Afterward, beads were washed three times with washing buffer [30 mM Tris (pH 7.4), 150 mM NaCl] resuspended in 30 μL 4X NuPAGE sample buffer (Invitrogen) containing 0.25 mM DTT (Roth), and bound proteins were eluted by boiling at 95 °C for 5 min.

In the case of competition assays, Sf9 cell lysates were incubated in the presence of various concentrations of the following peptides: LFNIKA**R**-AS**S**SPVILVGT in either nonphosphorylated or serine-phosphorylated form. Samples were separated on NuPAGE 4–12% gradient gels (Invitrogen), and the presence of LRRK2 Δ967 in the pull-down experiment was analyzed by Western blotting with anti–Strep-HRP conjugate (IBA) at a dilution of 100,000 in TBS-T with 2% (wt/vol) BSA for 1 h at room temperature. Subsequently, Western blot membranes were incubated with GST antibody (GenScript) or 14-3-3 (pan) antibody [Cell Signaling; dilution: 1/1,000 in TBS-T with 5% (wt/vol) BSA, overnight at 4 °C] to demonstrate equal protein loading.

FP. To investigate the binding of 14-3-3 isoforms to LRRK2, we used a direct FP assay. For peptide phosphorylation, 20 nM of the fluorescein-labeled LRRK2 peptides [S-LRRK2-1444 LFNIKARAS**S**SPVILVGT (S1444 bold and underlined), pS-LRRK2-1444 LFNIKARAS**p**S**S**SPVILVGT, LRRK2-R1441G LFNIKA**G**ASSSPVILVGT, and LRRK2-S1444A LFNIKARAS**A**SPVILVGT] was incubated with or without 500 nM PKA in 20 mM 4-morpholinopropanesulfonic acid (MOPS) (pH 7), 150 mM NaCl, 0.05% (vol/vol) CHAPS, 1 mM ATP, and 10 mM $MgCl_2$ for 4 h at 37 °C. As a control, the assay was performed in the presence of PKI (1 μM), purified from *E. coli* as described in Thomas et al. (53). For FP measurements, peptide at a final concentration of 10 nM was mixed with 2 μM 14-3-3 (gamma, theta, or zeta) in 150 mM NaCl, 20 mM MOPS, 0.005% (vol/vol) CHAPS using a FusionTM α-FP plate reader at room temperature for 2 s at Ex 485 nm/Em 535 nm in a 384-well microtiter plate (OptiPlate, black; PerkinElmer). Data were analyzed with GraphPad Prism 6.01 (GraphPad Software). Data presented in each graph are the mean ± SEM of triplicate measurements.

To determine the affinity between the 14-3-3 isoforms and phosphorylated and nonphosphorylated fluorescein-labeled LRRK2 peptide, increasing concentrations of GST–14-3-3 protein (from 1 nM to 100 μM) were mixed with 10 nM fluorescently labeled LRRK2 peptide as described above. Data presented in each graph are the mean ± SEM of triplicate measurements ($n = 3$ per data point) for a single experiment. K_d was determined with GraphPad Prism by plotting the fluorescence polarization signal against the logarithm of the 14-3-3 protein concentration and fitting a sigmoidal dose–response.

SPR. A Biacore 3000 instrument (GE Healthcare Biacore) was used to study the interaction of biotinylated LRRK2 peptides and 14-3-3 proteins. A Biotin CAPture kit (GE Healthcare Biacore) was used according to the manual. On the CAP sensor chip (carboxymethylated dextran matrix with ssDNA molecule preimmobilized) 3,700 response units were captured. Then, 60 nM peptide (flow 5 μL/min; injection of 5 μL corresponds to 80 response units) was immobilized via a biotin linker to the Biotin CAPture reagent sensor surface. A reference surface was saturated with biotin capture reagent without peptide, and the response was subtracted. All interaction experiments were performed at room temperature in running buffer [20 mM MOPS (pH 7), 150 mM NaCl, 0.005% surfactant P20] at a flow rate of 30 μL/min. After injection of 1 μM 14-3-3 over the surfaces (2 min), the dissociation phase was monitored for 2 min. Sensor surfaces were regenerated by injection of 6 M guanidine hydrochloride/150 μM sodium hydroxide.

ACKNOWLEDGMENTS. We thank Irmtraud Hammerl-Witzel, Melanie Spieker, and Hannah Breitenstein for expert technical assistance; Mira Sastri and Ralph Telgmann for critical reading of the manuscript; Mandy Diskar for helpful suggestions in cell culture; and Jörg D. Hoheisel for his support in the Affinomics project. This work was supported by European Union FP7 Health Programme, 241481 AFFINOMICS (to M.U., F.W.H., and A.J.); the Federal Ministry of Education and Research, fund number: 0316177F No Pain (to F.W.H.); the Otto–Braun–Fonds of the University of Kassel (K.M.); the National Genome Research Framework program NGFN-Plus, fund number: 01GS08140/subproject 12 (to M.U.); and the Michael J. Fox Foundation (C.J.G., M.U., and A.G.).

1. Moore DJ, West AB, Dawson VL, Dawson TM (2005) Molecular pathophysiology of Parkinson disease. *Annu Rev Neurosci* 28:57–87.
2. Mills RD, Mulhern TD, Cheng HC, Culvenor JG (2012) Analysis of LRRK2 accessory repeat domains: Prediction of repeat length, number and sites of Parkinson's disease mutations. *Biochem Soc Trans* 40(5):1086–1089.
3. Mata IF, Wedemeyer WJ, Farrer MJ, Taylor JP, Gallo KA (2006) LRRK2 in Parkinson's disease: Protein domains and functional insights. *Trends Neurosci* 29(5): 286–293.
4. Haugarvoll K, Wszolek ZK (2009) Clinical features of LRRK2 parkinsonism. *Parkinsonism Relat Disord* 15(Suppl 3):S205–S208.
5. Sheng Z, et al. (2012) Ser1292 autophosphorylation is an indicator of LRRK2 kinase activity and contributes to the cellular effects of PD mutations. *Sci Transl Med* 4(164): 164ra161.
6. West AB, et al. (2005) Parkinson's disease-associated mutations in leucine-rich repeat kinase 2 augment kinase activity. *Proc Natl Acad Sci USA* 102(46):16842–16847.
7. Gloeckner CJ, et al. (2010) Phosphopeptide analysis reveals two discrete clusters of phosphorylation in the N-terminus and the Roc domain of the Parkinson-disease associated protein kinase LRRK2. *J Proteome Res* 9(4):1738–1745.
8. Zach S, Felk S, Gillardon F (2010) Signal transduction protein array analysis links LRRK2 to Ste20 kinases and PKC zeta that modulate neuronal plasticity. *PLoS One* 5(10): e13191.
9. West AB, et al. (2007) Parkinson's disease-associated mutations in LRRK2 link enhanced GTP-binding and kinase activities to neuronal toxicity. *Hum Mol Genet* 16(2): 223–232.
10. Dzamko N, et al. (2012) The IkappaB kinase family phosphorylates the Parkinson's disease kinase LRRK2 at Ser935 and Ser910 during Toll-like receptor signaling. *PLoS One* 7(6):e39132.
11. Ito G, et al. (2007) GTP binding is essential to the protein kinase activity of LRRK2, a causative gene product for familial Parkinson's disease. *Biochemistry* 46(5): 1380–1388.
12. Li X, et al. (2011) Phosphorylation-dependent 14-3-3 binding to LRRK2 is impaired by common mutations of familial Parkinson's disease. *PLoS One* 6(3):e17153.
13. Nguyen PV, Woo NH (2003) Regulation of hippocampal synaptic plasticity by cyclic AMP-dependent protein kinases. *Prog Neurobiol* 71(6):401–437.
14. Choi J, et al. (2002) Phosphorylation of stargazin by protein kinase A regulates its interaction with PSD-95. *J Biol Chem* 277(14):12359–12363.
15. Ehlers MD (2000) Reinsertion or degradation of AMPA receptors determined by activity-dependent endocytic sorting. *Neuron* 28(2):511–525.
16. Goldsmith BA, Abrams TW (1992) cAMP modulates multiple K+ currents, increasing spike duration and excitability in Aplysia sensory neurons. *Proc Natl Acad Sci USA* 89(23):11481–11485.
17. Wolf ME, Mangiavacchi S, Sun X (2003) Mechanisms by which dopamine receptors may influence synaptic plasticity. *Ann N Y Acad Sci* 1003:241–249.
18. Lobbestael E, Baekelandt V, Taymans JM (2012) Phosphorylation of LRRK2: From kinase to substrate. *Biochem Soc Trans* 40(5):1102–1110.
19. Nichols RJ, et al. (2010) 14-3-3 binding to LRRK2 is disrupted by multiple Parkinson's disease-associated mutations and regulates cytoplasmic localization. *Biochem J* 430(3):393–404.
20. Bridges D, Moorhead GB (2004) 14-3-3 proteins: A number of functions for a numbered protein. *Sci STKE* 2004(242):re10.
21. Yaffe MB (2002) How do 14-3-3 proteins work?—Gatekeeper phosphorylation and the molecular anvil hypothesis. *FEBS Lett* 513(1):53–57.
22. Fraser KB, et al. (2013) LRRK2 secretion in exosomes is regulated by 14-3-3. *Hum Mol Genet* 22(24):4988–5000.
23. Foote M, Zhou Y (2012) 14-3-3 proteins in neurological disorders. *Int J Biochem Mol Biol* 3(2):152–164.
24. Steinacker P, Aitken A, Otto M (2011) 14-3-3 proteins in neurodegeneration. *Semin Cell Dev Biol* 22(7):696–704.
25. Walsh DA, Ashby CD, Gonzalez C, Calkins D, Fischer EH (1971) Krebs EG: Purification and characterization of a protein inhibitor of adenosine 3′,5′-monophosphate-dependent protein kinases. *J Biol Chem* 246(7):1977–1985.
26. Kemp BE, Graves DJ, Benjamini E, Krebs EG (1977) Role of multiple basic residues in determining the substrate specificity of cyclic AMP-dependent protein kinase. *J Biol Chem* 252(14):4888–4894.
27. Hennrich ML, et al. (2013) Universal quantitative kinase assay based on diagonal SCX chromatography and stable isotope dimethyl labeling provides high-definition kinase consensus motifs for PKA and human Mps1. *J Proteome Res* 12(5):2214–2224.
28. Shabb JB (2001) Physiological substrates of cAMP-dependent protein kinase. *Chem Rev* 101(8):2381–2411.
29. Giles N, Forrest A, Gabrielli B (2003) 14-3-3 acts as an intramolecular bridge to regulate cdc25B localization and activity. *J Biol Chem* 278(31):28580–28587.
30. Yaffe MB, et al. (1997) The structural basis for 14-3-3:phosphopeptide binding specificity. *Cell* 91(7):961–971.
31. Anand VS, et al. (2009) Investigation of leucine-rich repeat kinase 2: Enzymological properties and novel assays. *FEBS J* 276(2):466–478.
32. Jaleel M, et al. (2007) LRRK2 phosphorylates moesin at threonine-558: Characterization of how Parkinson's disease mutants affect kinase activity. *Biochem J* 405(2): 307–317.
33. Webber PJ, et al. (2011) Autophosphorylation in the leucine-rich repeat kinase 2 (LRRK2) GTPase domain modifies kinase and GTP-binding activities. *J Mol Biol* 412(1): 94–110.
34. Cookson MR (2010) The role of leucine-rich repeat kinase 2 (LRRK2) in Parkinson's disease. *Nat Rev Neurosci* 11(12):791–797.
35. Seol W (2010) Biochemical and molecular features of LRRK2 and its pathophysiological roles in Parkinson's disease. *BMB Rep* 43(4):233–244.
36. Dhillon AS, et al. (2002) Cyclic AMP-dependent kinase regulates Raf-1 kinase mainly by phosphorylation of serine 259. *Mol Cell Biol* 22(10):3237–3246.
37. Pungaliya PP, et al. (2010) Identification and characterization of a leucine-rich repeat kinase 2 (LRRK2) consensus phosphorylation motif. *PLoS ONE* 5(10):e13672.
38. Ohta E, Kawakami F, Kubo M, Obata F (2011) LRRK2 directly phosphorylates Akt1 as a possible physiological substrate: Impairment of the kinase activity by Parkinson's disease-associated mutations. *FEBS Lett* 585(14):2165–2170.
39. Freed E, Symons M, Macdonald SG, McCormick F, Ruggieri R (1994) Binding of 14-3-3 proteins to the protein kinase Raf and effects on its activation. *Science* 265(5179): 1713–1716.
40. Reuther GW, Pendergast AM (1996) The roles of 14-3-3 proteins in signal transduction. *Vitam Horm* 52:149–175.
41. Dougherty MK, Morrison DK (2004) Unlocking the code of 14-3-3. *J Cell Sci* 117(Pt 10): 1875–1884.
42. Muslin AJ, Tanner JW, Allen PM, Shaw AS (1996) Interaction of 14-3-3 with signaling proteins is mediated by the recognition of phosphoserine. *Cell* 84(6):889–897.
43. Molzan M, Ottmann C (2012) Synergistic binding of the phosphorylated S233- and S259-binding sites of C-RAF to one 14-3-3ζ dimer. *J Mol Biol* 423(4):486–495.
44. Zhao J, Meyerkord CL, Du Y, Khuri FR, Fu H (2011) 14-3-3 proteins as potential therapeutic targets. *Semin Cell Dev Biol* 22(7):705–712.
45. Daniëls V, et al. (2011) Insight into the mode of action of the LRRK2 Y1699C pathogenic mutant. *J Neurochem* 116(2):304–315.
46. Tan Y, Demeter MR, Ruan H, Comb MJ (2000) BAD Ser-155 phosphorylation regulates BAD/Bcl-XL interaction and cell survival. *J Biol Chem* 275(33):25865–25869.
47. Tzivion G, Luo Z, Avruch J (1998) A dimeric 14-3-3 protein is an essential cofactor for Raf kinase activity. *Nature* 394(6688):88–92.
48. Gasper R, Meyer S, Gotthardt K, Sirajuddin M, Wittinghofer A (2009) It takes two to tango: Regulation of G proteins by dimerization. *Nat Rev Mol Cell Biol* 10(6):423–429.
49. Gloeckner CJ, et al. (2006) The Parkinson disease causing LRRK2 mutation I2020T is associated with increased kinase activity. *Hum Mol Genet* 15(2):223–232.
50. Gloeckner CJ, Boldt K, Schumacher A, Roepman R, Ueffing M (2007) A novel tandem affinity purification strategy for the efficient isolation and characterisation of native protein complexes. *Proteomics* 7(23):4228–4234.
51. Rittinger K, et al. (1999) Structural analysis of 14-3-3 phosphopeptide complexes identifies a dual role for the nuclear export signal of 14-3-3 in ligand binding. *Mol Cell Biol* 4(2):153–166.
52. Zimmermann B, Chiorini JA, Ma Y, Kotin RM, Herberg FW (1999) PrKX is a novel catalytic subunit of the cAMP-dependent protein kinase regulated by the regulatory subunit type I. *J Biol Chem* 274(9):5370–5378.
53. Thomas J, et al. (1991) Expression in Escherichia coli and characterization of the heat-stable inhibitor of the cAMP-dependent protein kinase. *J Biol Chem* 266(17): 10906–10911.